Metallurgical Examination of a Failed Automotive Helical Suspension Spring

Report Number: Y1234

Danie Els

22nd November 2024

LPD Lab Services Limited
Suite 1, D Building
Glenfield Business Park
Philips Road
Blackburn
Lancashire, BB1 5RZ
United Kingdom
www.lpdlabservices.co.uk
enquiries@lpdlabservices.co.uk
Tel 01254-676074
Fax 01254-278845

Contact Name – Client Company Name
Address
Postcode

1 Introduction

LPD Lab Services received a portion of a fractured automotive helical suspension spring for metallurgical examination in order to determine the root cause of failure. This report discusses the results of light optical microscopy (LOM), scanning electron microscopy (SEM), energy dispersive X-ray (EDX) analysis, metallography, hardness testing and chemical analysis performed on the received failed portion of the coil spring.

2 Sample Preparation/Method Details

Visual and low magnification optical examinations were performed on the fracture face, using a Leica MZ12 binocular zoom microscope. This facilitates the study of macro fracture features that would be too small for observation with the unaided eye and it can help to identify the failure mechanism, the fracture initiation point, and factors that contributed to the failure.

A transverse section from directly adjacent to the fracture face was encapsulated in conductive phenolic resin, metallographically polished and then etched in 3% nital. After examination of the fracture face by SEM, a longitudinal section through the fracture origin was prepared in the same manner. Examination of both sections was done at magnifications up to 500x using a Zeiss Axioskop-40 metallurgical microscope.

Scanning electron microscopy was carried out on the fracture face and on the metallographically prepared polished section from adjacent to the fracture, using a Philips XL30 equipped with a tungsten filament and an EDX analyser. Both secondary electron (SE) and backscattered electron (BSE) imaging modes were employed. SE imaging gives good topographical contrast of the samples surfaces whilst contrast differences seen in BSE imaging are generally signs of different average elemental compositions – heavy elements have a brighter contrast and light elements have a darker contrast. The examination was performed using a beam acceleration voltage of 20 keV.

EDX analysis in the SEM was done on the corrosion products on the external surface of the section from adjacent to the fracture in order to determine whether any aggressive species were present. EDX is a normalised semi-quantitative compositional analysis technique that detects X-rays emitted from the top few micrometres of the sample surface after interaction with the electron beam. The emitted X-rays are characteristic for each element present. Even though EDX does not indicate the chemical states of elements, it can sometimes provide a degree of compound information from relative atomic proportions.

Vickers hardness measurements were performed on the metallographically prepared transverse section, using a Vickers-Armstrong B59153 hardness tester with a 10 kg load. Testing was performed according to BS EN ISO 6507.

The coil spring material was chemically analysed by inductively coupled plasma optical emission spectroscopy (ICP-OES), combustion (for carbon and sulphur).

3 Results and Comments

3.1 Visual Examination

The received sample of the fractured spring is shown from two sides in Figure 1 and Figure 2, respectively. Fracture occurred almost one revolution away from the end of the coil and the fracture initiation point was orientated toward the end of the coil. The fracture face was orientated at 45° to the axis of the spring wire, which is typical of fracture in torsion.

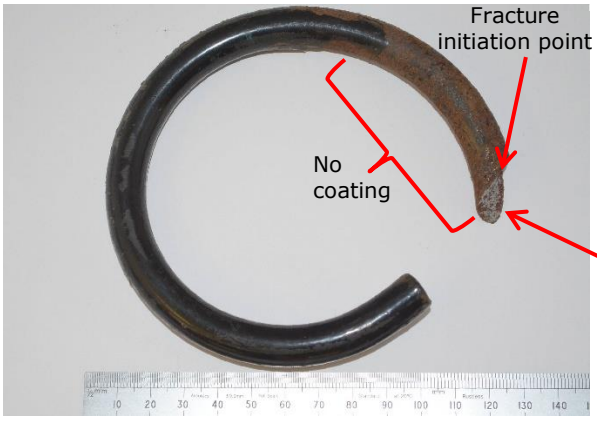

Figure 1. The received portion of the failed helical spring.

Figure 2. The opposite side to that shown in Figure 1.

All of the protective polymer coating was lost at the location of the fracture; up to about 9cm away from the fracture face, as indicated in the above images. The exposed steel surface had suffered a significant level of corrosion, having been exposed to spray water from salted road surfaces for a long time. Furthermore, the corrosion had propagated along the interface between the protective coating and the steel, pushing the coating away from the steel as it progressed, as shown in Figure 3. Corrosion products have a larger volume than the metal consumed in the corrosion process. The corrosion products will, therefore, push the coating outward, away from the metal surface. This action is termed corrosion jacking and can cause a coating to crack if it does not have sufficient elasticity.

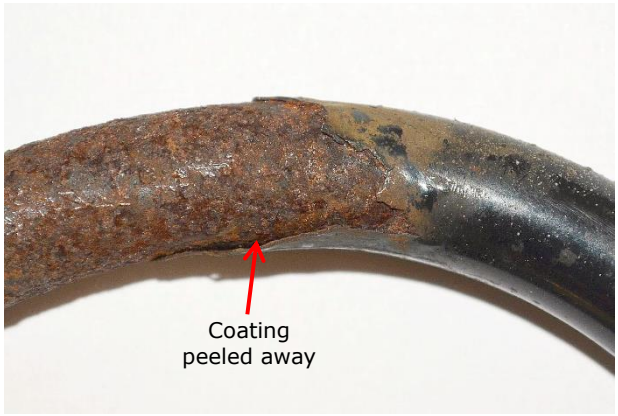

Figure 3. Corrosion progressed along the interface between the coating and the steel.

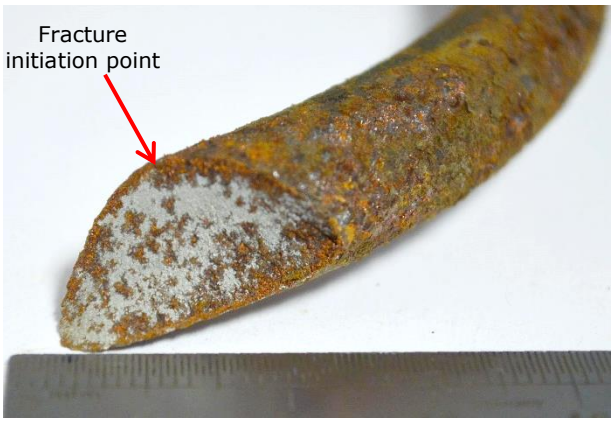

Figure 4. The fracture face with the location of the initiation point indicated.

3.2 Light Optical Microscopy

The fracture face suffered a significant level of corrosion after the failure had occurred. The reason for this was because the failure was discovered some time after it had occurred. Fortunately, the corrosive attack on the fracture face was patchy, leaving sufficient fractographic evidence for interpretation. Radial propagation lines on the fracture face confirmed that fracture initiated at the external surface, on the centreline radius (halfway between the outer curve and the inner curve of the helix), as indicated in Figure 1 and Figure 4.

A low magnification optical image of the fracture face is shown in Figure 5, with the fracture initiation point positioned at the top of the image. The fracture initiation point is shown at higher magnification in Figure 6. Unfortunately, all fractographic detail at the location of fracture initiation was spoiled by corrosion and the presence or absence of fatigue cracking could not be confirmed.

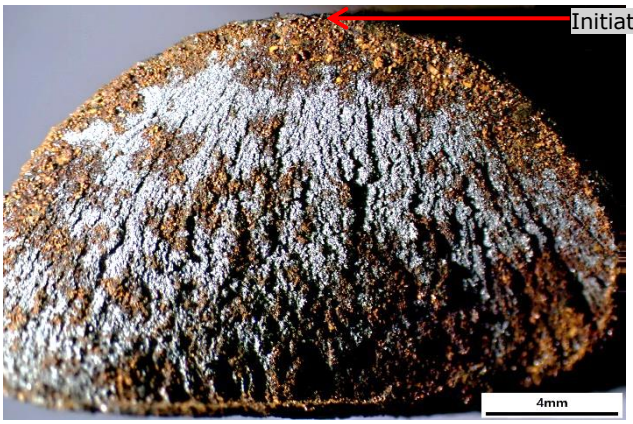

Figure 5. The fracture face illuminated from the side to accentuate the fractographic features.

Figure 6. The region of fracture initiation, spoiled by corrosion.

The external surface at the fracture initiation zone is shown in Figure 7. Due to damage caused by corrosion and because of the hindrance caused by the corrosion products, no evidence of a surface defect or surface irregularity that could have contributed to the fracture, could be observed on the external surface at the fracture initiation point. Figure 8 shows how the protective coating was lifted away from the spring surface.

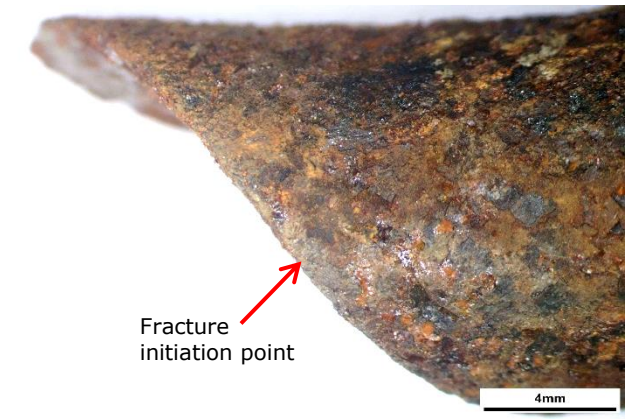

Figure 7. Fracture initiated at the bottom of the spring and propagated at an angle of 45° to the main axis of the spring wire.

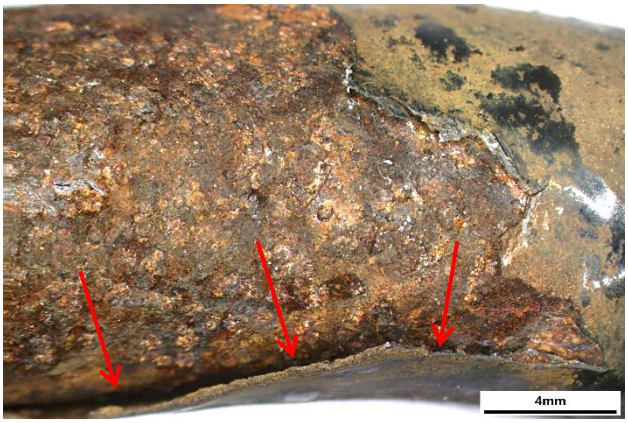

Figure 8. Corrosion progressed along the interface between the coating and the steel, peeling the coating off the spring.

3.3 SEM Examination & EDX Analysis

3.3.1 Cross-Section

The corrosion products on the external surface of the metallographically prepared cross-section from adjacent to the fracture face were analysed by EDX spectroscopy, in the polished condition (not chemically etched). Figure 9 shows a backscattered electron (BSE) image of the analysis location whilst Figure 10 shows the EDX spectra and extracted composition of the corrosion products.

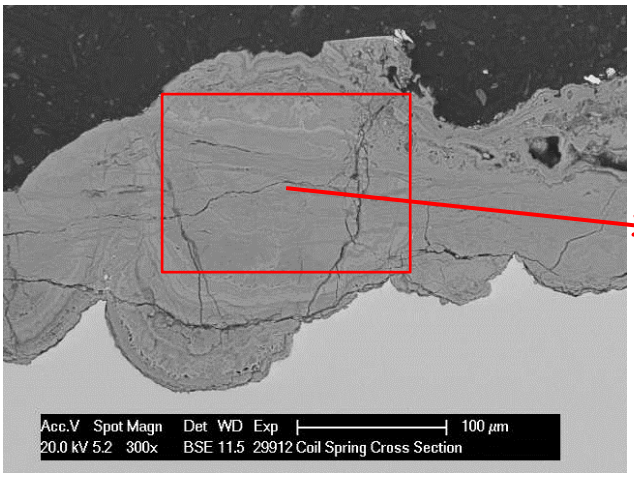

Figure 9. BSE image at the surface of the cross-section taken behind the fracture face.

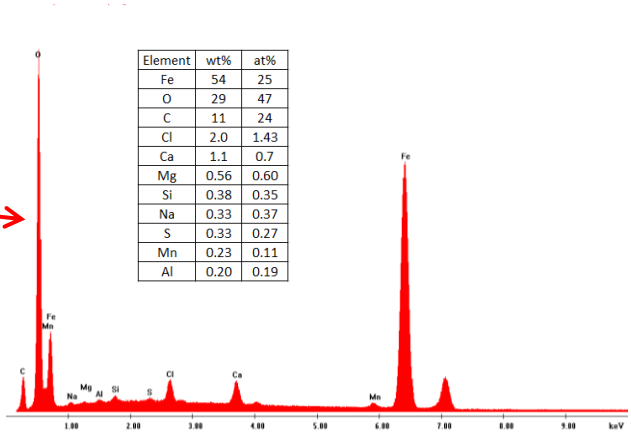

Element	wt%	at%
Fe	54	25
O	29	47
C	11	24
Cl	2.0	1.43
Ca	1.1	0.7
Mg	0.56	0.60
Si	0.38	0.35
Na	0.33	0.37
S	0.33	0.27
Mn	0.23	0.11
Al	0.20	0.19

Figure 10. EDX spectrum and composition of the corrosion products at the external surface.

The elements in the corrosion products strongly suggested corrosion by spray water from salted roads. The chlorine and sulphur would typically have originated from rock salt use for de-icing British roads in winter.

It should be borne in mind that adventitious carbon from exposure to the atmosphere adhering to the sample surface, along with fluorescence effects not compensated for by the models used in the ZAF correction software (which does not include overlayer effects), artificially increase the measured carbon concentration. The true surface carbon concentration measured by EDX is, therefore, always higher than the actual concentration.

3.4 Fracture Face

The high level of corrosion observed on the fracture face at the fracture initiation zone meant that the fractographic evidence at that location would have been spoiled. Any attempt to remove the corrosion products in order to study the underlying surface would have been in vain. Therefore, no chemical cleaning of the fracture face was undertaken. The fractographic examination focussed on the uncorroded regions of the fracture face.

A secondary electron (SE) image of an area of the fracture face just next to the corrosion products on the region of fracture initiation is shown in Figure 11 and a higher magnification SE image of the same area is shown in Figure 12. Fracture propagated entirely in a brittle, intergranular manner at this location. The fractographic features suggested hydrogen embrittlement cracking. There was no evidence of striation marks to confirm any action of fatigue cracking.

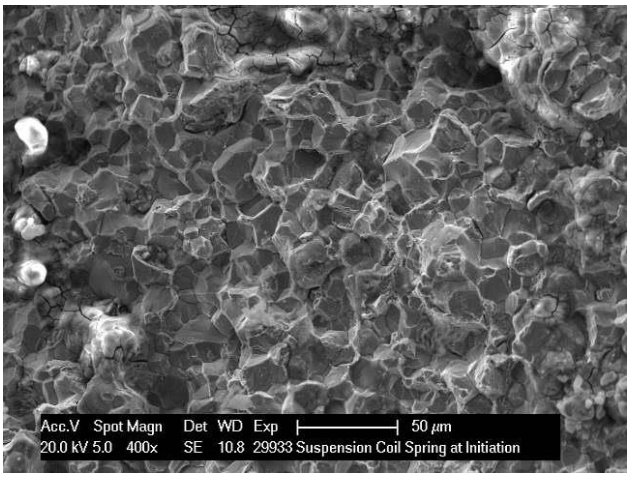

Figure 11. A lower magnification SE image of the fracture face just next to the corrosion products at the fracture initiation area.

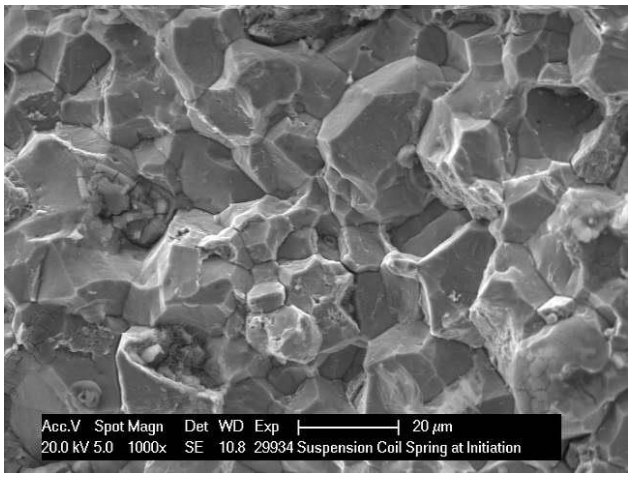

Figure 12. A higher magnification SE image of Figure 11 showing intergranular failure.

A secondary electron (SE) image of an area in the middle of the fracture is shown in Figure 13. Here, fracture mostly took place by micro-void coalescence (forming ductile dimples) and quasi-cleavage, as shown at higher magnification in Figure 14. Both are ductile failure mechanisms. There was also, however, evidence of brittle intergranular fracture and secondary cracking, as shown in Figure 15. This mixture of fracture mechanisms was due to the a significantly reduced hydrogen concentration away from the surface from where it would have diffused into the steel.

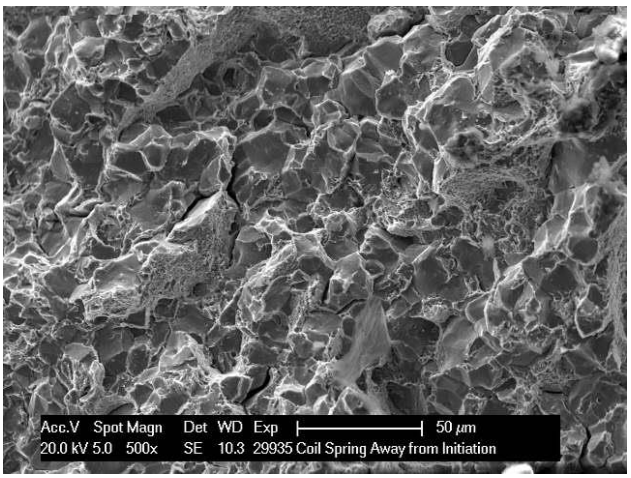

Figure 13. A lower magnification SE image of an area in the middle of the fracture face.

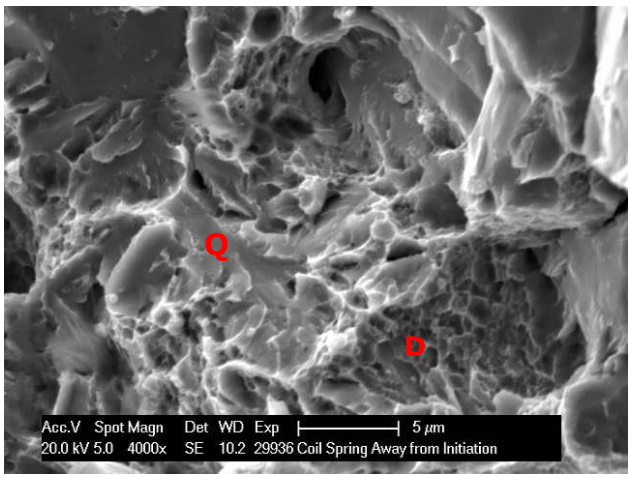

Figure 14. A higher magnification SE image of Figure 13 showing evidence of quasi-cleavage (Q) and ductile dimples (D).

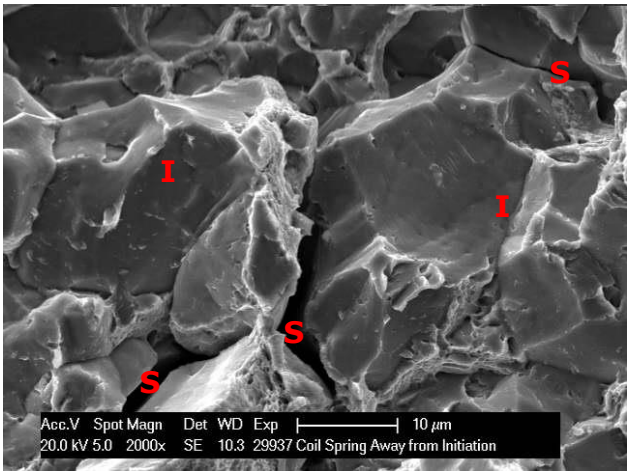

Figure 15. A higher magnification SE image of Figure 13 showing intergranular cracking (I) and secondary cracking (S).

3.5 Metallographic Examination

Examination of the metallographically polished section taken from behind the fracture face revealed that the entire external surface was affected by pitting corrosion, as showed in Figure 16. Some of the pits were as deep as 251 µm, as shown in Figure 17. These corrosion pits act as stress raisers that can facilitate the initiation cracks. There was no evidence of manufacturing defects (e.g., seams or laps).

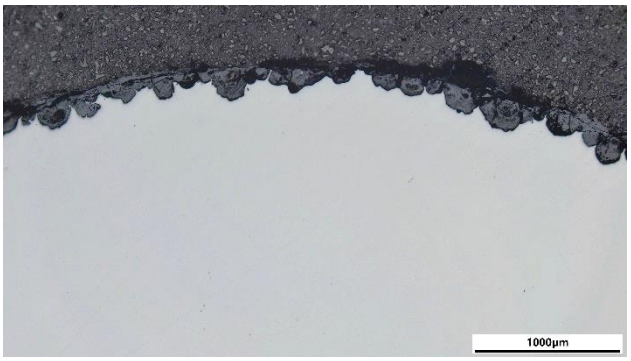

Figure 16. Optical image of the surface of the section taken from behind the fracture face.

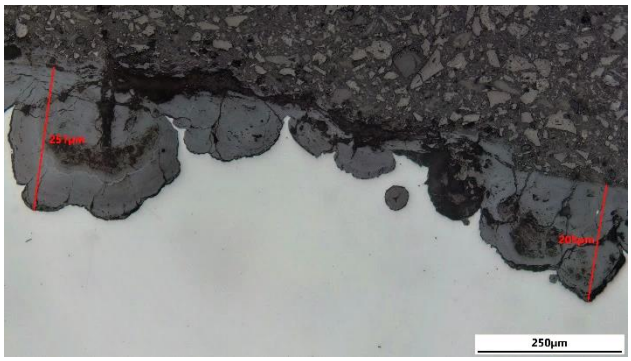

Figure 17. A higher magnification optical image of the pitting corrosion on the external surface.

Examination of the polished section taken through the fracture initiation area revealed numerous internal cracks at and near the fracture face, as shown in Figure 18. This typically was hydrogen induced cracking (HIC).

Examination of the etched section revealed that the material was in the quenched and tempered condition with a microstructure consisting of fine tempered martensite, as shown in Figure 19. There was no evidence of decarburisation, excessive non-metallic inclusions or defects.

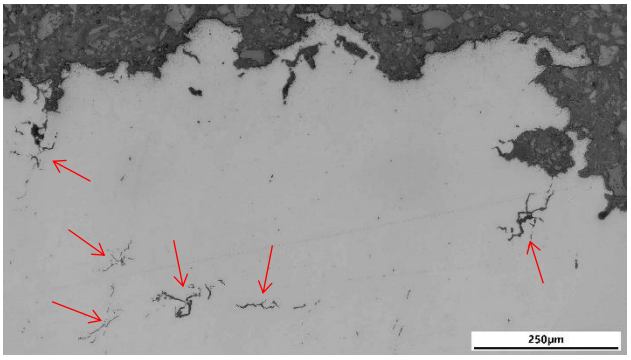

Figure 18. Hydrogen stress cracks at middle of fracture face, indicated by arrows.

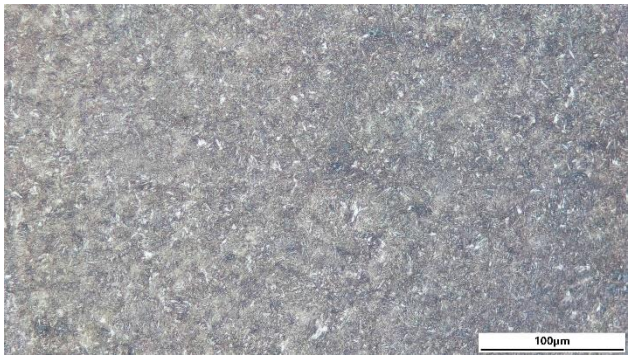

Figure 19. Microstructure of the polished and etched spring material.

3.6 Chemical Compositional Analysis

The chemical analysis results of the spring material and a reference specification are presented in Table 1. The composition was typical of a conventional spring steel material such AISI/SAE 5160. This material is well-suited for leaf and coil springs due to its potential toughness and durability.

Table 1. Spring chemical analysis results (wt%).

Element	**Coil Spring**	**ASTM A29 Grade 5160**
Carbon	0.60	0.56 – 0.61
Silicon	0.23	0.15 – 0.35
Manganese	0.76	0.75 – 1.00
Phosphorous	0.011	0.035 max
Sulphur	0.025	0.040 max
Chromium	0.90	0.70 – 0.90
Molybdenum	0.11	–
Nickel	0.23	–
Copper	0.076	–
Aluminium	0.020	–
Titanium	<0.01	–
Vanadium	<0.01	–
Niobium	<0.01	–
Calcium	<0.01	–

3.7 Hardness Testing

Table 2 presents results of the hardness tests done at half radius on the metallographically polished cross-section taken adjacent to the fracture. The results were acceptable for spring steel. AISI/SAE 5160 spring steel is typically specified to have a Rockwell hardness of around 52-56 HRC (544-613 HV) after heat treatment.

Table 2. Results of the hardness tests (Vickers 10 kg).

Test	Value (HV10)	Converted to HRC
1	545	52
2	545	52
3	542	52
Average	544	52

4 Conclusions

The coil spring failed by a mechanism known as corrosion hydrogen embrittlement and hydrogen induced cracking. No evidence of fatigue cracking was observed.

All of the protective polymer coating was lost at the fracture and the exposed steel surface had suffered significant corrosion. Sulphur as detected in the corrosion products and this would have originated from rock salt used for de-icing roads in winter. Sulphides are a well-known cathodic poison that prevent the combination of hydrogen ions, which are evolved by the cathodic corrosion reaction, to form hydrogen gas. The adsorbed hydrogen ions then diffuse into the steel and embrittle it. Even trace amounts of sulphides can significantly increase the absorption of hydrogen into high-strength steels.

Hard spring materials are very notch sensitive and the corrosion pits that formed at the surface would have acted as stress raising points from where cracking would have initiated. Therefore, one of the challenges for suspension springs is to protect them against corrosion. Powder coatings are frequently used as a corrosion prevention measure, but it is difficult to avoid damage to these coatings over a long time. Any breach in the protective coating will allow the underlying steel to corrode and the corrosion will spread along the interface between the coating and the steel.

In summary, the primary cause of the failure was a breach of the corrosion protective layer. This in turn led to corrosion, which liberated hydrogen, which entered the high strength steel, which embrittled it, which led to the fracture.

Primary Author: Danie Els MSc MIMMM
Function: Senior Metallurgist

Signature: _____
(hard copy only)

End of report